THESIS OF THE DOCTORAL (PhD) DISSERTATION

HUNGARIAN UNIVERSITY OF AGRICULTURE AND LIFE SCIENCES

DOCTORAL SCHOOL OF ANIMAL SCIENCE

INSTITUTE OF ANIMAL PHYSIOLOGY AND NUTRITION

The Head of Doctoral (PhD) School:

PROF. DR. ANDRÁS SZABÓ, DSc

Supervisor:

PROF. DR. ANDRÁS SZABÓ, DSc

FUMONISIN B SERIES' IMPLICATIONS ON BIOMEMBRANES' FATTY ACID COMPOSITIONS OF SPECIFIC TISSUES FROM RATS, SWINE AND RABBITS

DOI: 10.54598/004510

Written by:

OMERALFAROUG ABDALLA IBRAHIM ALI

Kaposvár
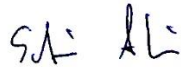
2024

Doctoral School of Animal Science

Name: OMERALFAROUG ABDALLA IBRAHIM ALI

Discipline: Animal Physiology and Health

Head: Prof. Dr. András Szabó, DSc

                MATE, Institute of Animal Physiology and Nutrition

                Department of Animal Physiology and Health

Supervisor: Prof. Dr. András Szabó, DSc

                MATE, Institute of Animal Physiology and Nutrition

                Department of Animal Physiology and Health

....

Approval of the Head of Doctoral School   Approval of the Supervisor(s)

*(**NB**: The doctoral dissertation has to be submitted in four copies bound with the original signatures and the ten theses with the photocopied signatures to the Office of the PhD School concerned.)*

1. RESEARCH BACKGROUND AND OBJECTIVES

Mycotoxins were discovered earlier, in the medieval period, as demonstrated by the recognition of ergot, which implicated a toxicological disease referred to as St. Anthony's fire (Bennett and Klich, 2003). Upon then, these compounds have received a great deal of attention, with a focus on their identification and biological impacts. To date, around 500,000 secondary metabolic products have been indexed in databases, among which 15,600 are derived from fungi (Bills and Gloer, 2016). Notably, a collection of various genera of fungi have been identified to contribute to these metabolites; however, specific genera like *Aspergilli*, *Fusaria*, *Penicillium, Alternaria*, and *Claviceps* have received increased attention, primarily due to their acknowledged mycotoxigenic activities (El-Sayed et al., 2022; Pandey et al., 2023). *Fusarium* species are highly prevalent in soil and food/feed crops, where they produce fusariotoxins, a family of secondary toxic metabolites produced by the genus *Fusarium*, notably including trichothecenes (such as deoxynivalenol (DON) and T-2 toxin), fumonisins (FUMs), zearalenone (ZEN), emerging mycotoxins (e.g., enniatins, beauvericin, fusaproliferin, and fusaric acid), and other mycotoxins. DON, ZEN, FUMs, and T-2 are apparently the most prevalent and studied mycotoxins worldwide, demonstrating 70%, 59%, 57%, and 15% prevalence risk, respectively, with an overall mycotoxin detection rate of 99% among all samples (dsm-firmenich, 2023). These toxins vary in their structures and, consequently, their toxic-active molecules/groups, which define their modes of action and target animal species and within those organs/tissues.

FUMs represent a category of mycotoxins that are non-fluorescent and primarily synthesized by specific fungi, predominantly *Fusarium* species. Considerable concerns have been expressed worldwide, emphasizing its high prevalence and toxic effects (evident and potential) in plants, animals, and humans (Rheeder et al., 2002). A large number of FUM isomers have been identified to date that vary in their degree of toxicity. FUM B_1 (FB_1) is, in fact, the most toxic structure of FUMs, displaying numerous adverse effects on vertebrates (Voss and Riley, 2013). This phenomenon of FUM toxicity is academically referred to as the "fumonisin paradox", a term coined to describe the riddle status surrounding the diminished bioavailability of FUM (3-5%) compared to its potent toxic effect (Shier, 2000). Among the dynamic ranges of toxicity caused by FUM is the disruption of cellular membranes. This perturbation is primarily attributed to its interference with sphingolipid metabolism, resulting in competition with ceramide synthase (CerS), a key enzyme involved in the metabolism of sphingolipids. This mechanism displays specific features, including the proportional

increase of sphinganine (Sa) and, to a lesser extent, liberated sphingosine (So) (Riley and Merrill, 2019). The disruption of sphingolipid metabolism induced by FUMs is crucial, leading to modifications in the composition of membrane lipids and, consequently, the disintegration of cell membranes (Burger et al., 2018).

To date, a few *in vitro*-based studies have investigated the disruption of membrane lipids by FB_1; however, these studies reported relatively drastic effects of toxin doses known to trigger cancer. These studies unutilized rat hepatocytes and cancer cells in their design. Further *in vivo* studies employing the same toxin doses are also available, reporting, to some extent, discrepancies between *in vitro* and *in vivo* models in rat liver. It is obvious that the rat model was the most utilized, whereas scarce investigations have been carried out on swine (liver, kidney, and lung) and rabbits (erythrocytes). Therefore, the existing literature might be considered somewhat inadequate, especially concerning swine and rabbits. Thus, further studies are necessary to confirm the reported alterations. In addition, there is a noticeable gap in the approach to dose- and time-dependent effects. Even though various dose paradigms were employed in the previously mentioned studies, no dose-response relationship was reported in relation to membrane fatty acids. Moreover, multiple studies have reported the effect of FB_1 on the male genital system, but no report has yet determined the magnitude of its toxicity on the fatty acid composition of the membranes of male reproductive tissues. Thus, it would be intriguing to investigate the following points in a sequential experimental plan, which are directly related to the dissertation of the doctorate:

1. Evaluation of the potential disruption caused by FBs to cellular membranes across different tissues and species, with a primary focus on cellular integrity.
2. Examination of the consequences of FBs on rats, swine, and rabbits, primarily focusing on the dose- and time-dependent response of fatty acids.
3. Investigation of the influence of FBs on the cation flux enzymatic regulation of erythrocytes in swine.
4. Determination of the potential induction of lipid peroxidation by FBs and its contribution to the final composition of membrane fatty acids.

2. MATERIALS AND METHODS

2.1. Mycotoxins

A pure FB_1 was obtained from Merck-Sigma-Aldrich (Schnelldorf, Germany). For the production of FBs (FB_{1+2+3}), the fungal strain *Fusarium verticillioides* (MRC 826) was inoculated on pre-soaked, sterile maize kernels, in the form of spore suspension. The incubation was set to 25 °C for 5 weeks, and the final FBs concentration in dried culture material was harvested in different production batches. Details on fungal culture preparation were published earlier (Fodor et al., 2006). The content of FBs was determined by the LC-MS-2020 (Shimadzu, Kyoto, Japan) (Fliszár-Nyúl et al., 2022). In the case of oral mycotoxin administrations (though diet), the absence of FBs co-occurrence with deoxynivalenol (DON), zearalenone (ZEN), and T-2 toxin has been confirmed, in which the analyzed diets did not contain detectable concentrations (below the limit of detection; 0.053, 0.005, and 0.011 mg/kg for DON, ZEN, and T-2 toxin, respectively).

2.2. Animals, experimental design and sample collections

2.2.1. Study on rats

Adult male Wistar Crl:WI BR rats (8 weeks of age at the beginning) were enrolled in the study and were kept in metabolic cages (Tecniplast, Castronno, Italy) individually. The animals (n = 6 in each group, total n = 48) were fed Ssniff R/M-Z + H feed (Ssniff GmbH, Soest, Germany). The rats were kept in a 12-h light and 12-h dark daily rhythm, at 20 °C in a rodent room, with a relative air humidity of 50%. Feed was offered *ad libitum,* and feed intake was measured daily. Increasing concentrations of FB_1 (0, 20, 50, and 100 mg kg^{-1} diet, expressed as feed dose equivalent) were tested in a short and then a longer-term experiment (5 and 10 days, respectively). The pure mycotoxin was purchased from Merck-Sigma-Aldrich (Schnelldorf, Germany), and stock solutions were prepared with sterile physiological salt solution. The solutions contained the daily toxin dose in exactly 1 ml, and this solution was administered as a single intraperitoneal dose. For the control animals, 1 ml of sterile physiological salt solution was dosed. Mycotoxin treatment was set as follows: 36 µg per animal day^{-1} (approx. 120 µg kg^{-1} body weight (BW) day^{-1}), 90 µg per animal day^{-1} (approx. 300 µg kg^{-1} BW day^{-1}) and 180 µg per animal day^{-1} (approx. 600 µg kg^{-1} BW day^{-1}). Calculating with the average feed intake of 30 g per animal day^{-1} and the absorption ratio of the toxin (Martinez-Larranaga et al. 1999), the intraperitoneal (i.p.) administration represented the following dietary exposures: approx. 20, 50, and 100 mg kg^{-1} dietary equivalent for FB_1. The two, basically similar treatments lasted for 5 (n = 24) and 10 days (n = 24), respectively, with only the exposure time being different. On days 6

and 11, after taking blood from the retro-orbital plexus, the animals were sacrificed by cervical dislocation and were immediately dissected.

The experimental protocol was authorised by the Food Chain Safety and Animal Health Directorate of the Somogy County Agricultural Office, under the permission number SOI/31/00308-10/2017.

2.2.2. Study on piglets

Altogether, 3 x 6 weaned Danbred piglets were enrolled in the study at the age of 35 days. The piglets were caged individually in 80 x 80 cm metabolic cages. After a 14-day adaptation (at the exact age of 49 days) period, the duration of the feeding trial was 21 days. While the control is toxin free, one group was fed a piglet diet complemented with 15 mg FBs/kg diet (contaminated by a fungal culture), whereas another group was fed 30 mg FBs/kg. The diet was offered twice a day, in equal proportions (equivalent to 0.5 kg feed consumption/animal/day during the first week and gradually increased to reach 0.7 kg feed intake/animal/day at the last week). At the end of each day, the feed residual was measured back for the daily feed intake determination. During the whole study, water was offered ad libitum to the piglets via automatic drinkers. The house's environmental conditions (such as temperature and humidity) were adjusted to meet the needs of weaned piglets. At the end of the trial, the piglet's body weight was determined individually. Later on, the piglets were euthanized by exsanguination after sedation (Euthanyl-Pentobarbital Sodium, 400 mg/mL, Dechra Veterinary Products, Shrewsbury, UK), and their blood, liver and lung were sampled for analysis. Collected samples were immediately stored at $-80\ °C$ for further analysis.

The experiments were carried out according to the regulations of the Hungarian Animal Protection Act. The allowance number for the studies was SOI/31/00308-10/2017 (date of approval: 28 February 2017, by the Hungarian National Scientific Ethical Committee on Animal Experimentation, and issued on 27 March 2017 by the Somogy County Government Office, Department of Food Chain Safety and Animal Health).

2.2.3. Study on rabbits

Altogether, 3×10 Pannon White rabbit bucks were enrolled in the study at the starting age of 24 weeks. The animals were already in production and underwent sperm collection weekly, as well as once before the study. The rabbits were fed on a commercial buck diet free of medications. A *Fusarium verticillioides* fungal culture of high FB_1 concentration was mixed into the ration of the experimental animals, so as to provide a daily FBs feed concentration of 10 and 20 mg/kg. BW and feed intake (FI) were recorded throughout the experimental period. Feed was offered *ad libitum*, as

was drinking water from nipple drinkers. The rabbits were caged individually in a rabbit stable in controlled environment, whereby the photoperiod was natural in the stable (2018, October–November). The study lasted for a total of 65 days, and on day 67, animals were euthanized by exsanguination after sedation (Euthanyl-Pentobarbital Sodium, 400 mg/mL, Dechra Veterinary Products, Shrewsbury, UK), and splanchnic organs, testes, and blood were sampled. During the study period, altogether five times, sperm samples were taken for cell integrity and viability analysis. Ejaculate collection was performed with water (37 °C) filled artificial vaginas having a collection tube as an attachment, performed by the caretaker, using a rabbit fur as a phantom. The collection tubes were immediately incubated at 37 °C.

The experiments were carried out according to the regulations of the Hungarian Animal Protection Act. The allowance number for the studies was SOI/31/00308-10/2017 (date of approval: 27 March, 2017).

2.3. Lipid analysis

2.3.1. Total lipid extraction

Samples of livers, kidneys, and lungs (after frozen storage at −20°C) were homogenised (IKA T25 Digital Ultra Turrax, Staufen, Germany) in 20-fold volume of chloroform:methanol (2:1 *v:v*) and total lipid content (complex lipids) was extracted according to Folch et al. (1957). Solvents were ultrapure-grade (Merck-Sigma-Aldrich, Schnelldorf, Germany) and 0.01% butylated hydroxytoluene was added to prevent fatty acid oxidation. With regard to piglets' red blood cells (RBCs), the RBC ghost moiety (i.e., porous, lysed cells) not used for enzyme assay was directly lipid-extracted according to the method of Folch et al. (1957). The same extraction method has been performed on testes and sperms, whereas the latter fraction was prepared from collected semen by 3× washing in 10-fold volume of phosphate buffered saline, and the washed cells were extracted (to gain complex lipids).

2.3.2. Separation of different lipid fractions

The lipid extracted from lysed porcine RBCs did not undergo separation. However, in respect to rabbit samples, total phospholipids have been extracted via glass chromatographic columns, containing 300 mg of silica gel (230–400 mesh) for 10 mg of total lipids (Leray et al., 1987). Neutral lipids were eluted with 10 mL chloroform for the above fat amount, then 15 mL acetone:methanol (9:1 *v:v*) was added, while 10 mL pure methanol eluted the total phospholipids.

For the separation of phospholipid classes, thin layer chromatography (TLC) was used. Extracted complex lipids were spotted onto pre-dried (110 °C, 2 h) 20 × 20 cm TLC plates (Merk-Sigma-Aldrich

Cat. No.: 99570). In the case of rat samples, the separation was performed in one dimension, using the eluent mixture of chloroform:methanol:water (25:10:1 *v/v/v*), developing the plate until the top, in an all-glass, covered, TLC chamber (Christie, 2003). Concerning samples from nursery piglets, the eluent mixture was methyl acetate–isopropanol–chloroform–methanol–aqueous 0.025% KCl (25:25:25:10:9 *v/v/v/v/v*) (Heape et al., 1985). Primuline spray (5 mg in 100 ml of acetone:water (80:20, Merck-Sigma-Aldrich Cat. No.: 206865)) was used to stain lipid spots, and detection was performed under ultraviolet light (365 nm). To identify phospholipid classes, certified reference materials were used as follows: N-Acyl-D-sphingosine-1-phosphocholine (Merck-Sigma-Aldrich Cat. No. S0756), L-α-phosphatidylcholine (Merck-Sigma-Aldrich Cat. No.: P3556), L-α-phosphatidylethanolamine (Merck-Sigma Cat. No.: P7943), L-α-phosphatidylserine (Merck-Sigma-Aldrich Cat. No. 870336C), and L-α-phosphatidylinositol (from Glycine max, Merck-Sigma-Aldrich Cat. No. P6636). Identified fractions were scraped off the plates and extracted 3 times into the TLC eluent mixture.

2.3.3. Transmethylation

Prepared/extracted fractions from piglets' RBCs and rabbits' testes and sperms were evaporated under a nitrogen stream and trans-methylated with a base-catalyzed $NaOCH_3$ method (Christie, 1982). Produced fatty acid methyl esters were extracted into 250 µL of ultrapure n-hexane for gas chromatography. However, acid-catalyzed method was employed for transmethylating the isolated lipid fractions from livers, kidneys, and lungs of piglets and/or rats. Their solvents were evaporated entirely, and lipids were trans-methylated with 1% H_2SO_4 in methanol (Christie, 2003). Fatty acid methyl esters were extracted into 150 µL of ultrapure n-hexane for gas chromatography.

2.3.4. Gas chromatography and data generation

The analysis of the prepared fatty acid methyl esters was performed on a GC-Shimadzu 2030 equipped with an AOC 20i automatic injector (Kyoto, Japan), a Phenomenex Zebron ZB-WAXplus capillary GC column (30 m × 0.25 mm ID, 0.25 µm film, Phenomenex Inc., Torrance, CA, USA), and a flame ionization detector (FID) detector. Characteristic operating conditions were: injector temperature: 220 °C; detector temperature: 250 °C; helium flow: 28 cm/sec. The oven temperature was graded: from 60 (2 min hold) to 150 °C, from 150 to 180 °C: 2 °C/min and 10 min at 180 °C, from 180 to 220 °C: 2 °C/min, and 16 min at 220 °C. The makeup gas was nitrogen.

To identify individual fatty acids, an authentic external fatty acid standard mixture (Merck-Sigma-Aldrich, Schnelldorf, Germany) was used. Fatty acid results were expressed as weight % of total fatty

acid methyl esters. The unsaturation index (UI) was calculated to express the number of double bonds in 100 fatty acid chains. Calculation was performed with the LabSolutions 5.93 software, using the PostRun module (Shimadzu, Kyoto, Japan) with manual peak integration.

2.4. Erythrocyte's "Ghost" preparation

Fresh venous blood was sampled into heparinized (20 IU/mL whole blood) tubes and was centrifuged for 10 min at 1000 g (SIGMA 3-30KS refrigerated centrifuge, Osterode am Harz, Germany). Plasma and the buffy coat were removed, and the erythrocyte bulk was washed 3 times with 10 volumes of TRIS-HCl (0.1 M; pH = 7.4) at 4 °C. After each wash, the buffy coat (and the washing medium as supernatant) was siphoned. Red blood cell (RBC) lysis was induced by ice-cold hypotonic TRIS-HCl solution (15 mM; pH = 7.4). Erythrocyte lysate was centrifuged at 15,000 g for 10 min at 4 °C repeatedly, until the washing medium was colorless (~7 times). Washing medium hemoglobin content was controlled with spectrophotometry at 418 nm in 10 mm path length optical cuvettes against medium blank until 0.001 Abs value (Shimadzu UV160 spectrophotometer, Shimadzu, Kyoto, Japan). The original method was described by Shanmugasundaram et al. ([1992]). The protein content of the suspension was determined according to Lowry et al. ([1951]), with bovine serum albumin as a standard (Shimadzu UV1900 spectrophotometer, Shimadzu, Kyoto, Japan). The RBC ghosts were stored frozen (−70 °C) until analysis.

2.5. Determination of the erythrocyte Na⁺/K⁺ ATPase activity

For the assay procedure, a quantity equal to 300 µg protein was used. The relatively high quantity was reasoned by the fact that the abundance of the enzyme is relatively low in red cells (Djemli-Shipkolye et al., [2004]). RBC ghosts were pre-incubated (10 min at 37 °C) in an incubation medium (92 mM TRIS-HCl (pH 7.4), 100 mM NaCl, 20 mM KCl, 5 mM $MgCl_2$ and 1 mM EDTA) (Bedin et al., [2001]). The reaction was started by the addition of 6 mM vanadate free ATP (disodium salt, Merck-Sigma Aldrich A26209). Incubations (37 °C at 30 min) were performed in the presence (2 mM) and absence of ouabain, a specific Na⁺/K⁺ ATPase inhibitor (ouabain octahydrate, Merck-Sigma-Aldrich O3125). The reaction was stopped by addition of ice-cold trichloroacetic acid at a final concentration of 5%, and samples were centrifuged at 5000 g for 10 min at 4 °C. The phosphate liberation was determined from the supernatant and was given as the difference of the Pi liberation without and with ouabain, in nmol Pi/mg protein/h. The liberated Pi was measured photometrically (Shimadzu UV1900 spectrophotometer, Shimadzu, Kyoto, Japan), according to Hurst ([1964]), in 10 mm path length optical glass cuvettes (Hellma Optik GmbH, Jena, Germany). All assays were performed in triplicate, and

blanks were included in each run to determine the endogenous phosphate concentration and the non-enzymatic ATP breakdown (i.e. Pi liberation). The amount of phosphate was read from the standard curve prepared using known concentrations of KH_2PO_4, according to Bełtowski and Wójcicka (2002). To ascertain that the ATP concentration in the medium is reaching the level of enzyme saturation, a simple test was performed, namely, the doubling of the enzyme quantity doubled the apparent enzyme activity, while the doubling of the ATP concentration did not alter it.

2.6. Evaluation of sperm viability

Fresh semen samples were immediately transferred to the laboratory at 37 °C. Flow cytometry was performed with a Molecular Probes Inc. (Eugene, OR, USA) LIVE/DEAD sperm Viability Kit (L-7011) containing SYBR14 and propidium iodide (PI). The staining protocol followed the description of Nagy et al. (2003). In brief, 100 nM SYBR 14 working solution (Component A of the LIVE/DEAD Sperm Viability Kit, diluted 10-fold with dimethyl sulfoxide 10 μl), and 2.4 mM PI stock solution (undiluted Component B of LIVE/DEAD Sperm Viability Kit, 2 μl) were added to 1 mL sperm (extended to approximately 1×10^6/mL in pre-warmed phosphate buffered saline). Samples were incubated at 37 °C for 10 min in darkness. The samples were transferred immediately after incubation for flow cytometric analysis. A Partec CyFlow Space equipment (Sysmex Partec GmbH, Görlitz, Germany) was operated with the FloMax software (ver. 2.9.), with a two-laser design (20 mW at 488 nm blue solid-state laser and a 40 mW at 635 nm red diode laser). The flow speed was 25 μl sec^{-1}, and acquisitions were stopped after recording 5000 total events. SYBR14 fluorescence (FL) intensity was recorded on detector FL1 (green), while PI fluorescence intensity was recorded on detector FL3 (red), on a log scale. Data files were stored in standard FCS file format. Flow cytometric results were evaluated with the FloMax software (ver. 2.9., Partec GmbH, Görlitz, Germany), and the live/dead cell ratio expressed as % was handled as the end result.

2.7. Antioxidant Status and Lipid Peroxidation

For the determination of lipid peroxidation and antioxidant status, whole tissue samples were stored at −70 °C until analysis. Lipid peroxidation was assessed with the determination of thiobarbituric acid reactive substances and expressed as malondialdehyde (MDA), which was served as standard (Placer et al., 1966) in the 10-fold volume of tissue homogenate in physiological saline (0.65 w/v% NaCl). The amount of glutathione (GSH) and glutathione peroxidase (GSHPx) activity was measured in the 10,000× g supernatant fraction of tissue homogenate. The quantification of the GSH was performed according to the method of Rahman et al. (2006) using 5,5′-dithiobis-2-nitrobenzoic acid (DTNB) as

a sulfhydryl reagent to form a yellow derivative, which is measurable at 412 nm. The activity of GSHPx was determined according to Matkovics et al. (1988) by applying an end-point direct assay with GSH and cumene hydroperoxide as co-substrates. GSH concentration and GSHPx activity were calculated from the protein content of the 10,000× g supernatant fraction after centrifugation (10 min at 4 °C), which was measured by the Folin-phenol reagent (Lowry et al., 1951). In all instances, the color was measured with UV–Vis spectrophotometry in 10 mm threaded optical glass cuvettes.

2.8. Histopathology and microscopic sperm quality assessment

Tissue specimens were stored in 10% neutrally buffered formalin and were embedded into paraffin. For light microscopic analysis, microtome slides of five micrometers were prepared and stained with hematoxylin-eosin. The main pathological alterations have been described and scored according to their extent and severity as follows: 0 = no alteration, 1 = slight/small scale/few, 2 = medium degree/medium scale/medium number, and 3 = pronounced/extensive/numerous. The histopathological analysis was performed according to Act #2011 (03.30) of the Hungarian Ministry of Agriculture and Rural Development and was in accordance with the ethical guidelines of the OECD Good Laboratory Practice for Chemicals (1997).

The fresh semen samples were used for the preparation of smears. Smears were dried at room temperature and were stained after Feulgen with a staining kit (Merck-Sigma, Schnelldorf, Germany, Cat. No. 1079070001), according to Barth and Oko (1989). The smears were protected with cover plates using Entellan mounting medium (Merck–Sigma-Aldrich Cat. No. 1079600500), and the cell evaluation was based on visual counting (200 cells/smear) on digital images taken at 400× magnification with an Olympus CX-41 (Olympus, Tokyo, Japan) phase contrast microscope equipped with a digital camera.

2.9. Statistical data analysis

All data were tested for normality (Shapiro–Wilk test), whereas the extent of standard deviation was compared between groups with Levene's F test. After this, the univariate analysis of variance (ANOVA) was used on the control and total FB-fed group means, with the Least Significant Difference (LSD) "post hoc" test for detailed inter-group differences. However, the distribution of the different morphologic spermium groups was compared with the chi^2 probe. Spermatological variables gained from the five consecutive samplings, at each sampling time were compared with ANOVA; time–dependent alteration of the different three groups was tested with repeated measures analysis. For dose– and time–response determination, the Pearson correlation was calculated between the

offered doses of FB_1/FBs or sodium pump activities and further fatty acid variables, always using individual data-pairs. Identified p-values < 0.05 were subjected to linear regression analysis, whereas only R^2 greater than 0.55 are reported. The software that performed data evaluation was IBM SPSS 20. For significance level identification, the calculated probability of a p-value < 0.05 was set for all tests.

Principal Component Analysis (PCA) was performed on the fatty acid profile of the different phospholipids from livers and lungs with the Unscrambler 9.7. software to seek principal components describing the variance responsible for the "group formation" with the highest possible efficacy. The sole purpose of PCA was not to discriminate between certain groups of treatments based on their chemical composition, but rather to describe the basic orientation of the groups within the multidimensional space described by the variables investigated (e.g., fatty acid profile elements). The orientation of the samples is described by the score plot, which shows the scores of each sample along with the first two principal components. The variable impact is presented with the loadings bar graph, which shows the contribution of the variance of each investigated variable to the full variance of the first principal component; that is, the values of the loadings graph are the weights for each original variable when calculating the principal component.

3. RESULTS

3.1. Fumonisin B1 induced compositional modifications of the renal and hepatic membrane lipids in rats – dose and exposure time dependence

3.1.1. Dose- and time-response relationship of fatty acids to fumonisins

The potential dose response assessment has been performed on altered fatty acids in phosphatidylcholine (PC), phosphatidylethanolamine (PE), and phosphatidylinositol (PI) from livers and kidneys of rats. Among these phospholipid classes, the kidney PC showed the most responses, which were noticed after 5 and 10 days of exposure. Following 5 days, C16:0 (palmitic acid), C20:4 n6 (arachidonic acid, or AA), C22:6 n3 (docosahexaenoic acid, or DHA), total polyunsaturation (PUFA), total omega-3 (Σn3), and total omega-6 (Σn6), unsaturation index (UI) and average chain length (ACL) of PC fraction exhibited dose responses, whereas palmitic, C18:1 n9 (oleic acid), C20:1 n9 (gondoic acid), C20:3 n6 (dihomo-γ-linolenic acid, or DGLA), and total monounsaturation (MUFA) were providing linear results (Table 1). The kidney PI also exhibited linear fittings on days 5 and 10. The marked decrease in its unsaturation was underscored by the linear regression results, namely that stearic acid provided an accurate fit with positive slope, while the opposite was proven for PUFA. Furthermore, DGLA was the only fatty acid providing a dose response marked by a linear proportional depletion. The liver was less responsive, in which only Σn3 provided a linear fit.

Table 1. Characteristics of the linear dose response equations in the kidney and the liver lipid fractions (only cases with an R^2 value exceeding 0.6 are shown).

| Kidney PC	5 days				10 days			
	Compound	Slope	Constant	R^2	Compound	Slope	Constant	R^2
	C16:0	30.3	1.78	0.635	C16:0	0.156	0.108	0.639
	C20:4 n6	-2.74	21.6	0.639	C18:1 n9	1.359	2.565	0.721
	C22:6 n3	-0.198	1.24	0.672	C20:1 n9	0.082	0.027	0.733
	PUFA	-3.63	31.1	0.639	C20:3 n6	-0.238	1.193	0.628
	Σn3	-3.38	29.2	0.633	MUFA	1.413	3.02	0.719
	Σn6	-0.236	1.69	0.689				
	UI	-13.8	116.8	0.641				
	ACL	-0.106	17.9	0.656				
Kidney PI	**5 days**				**10 days**			
	Compound	Slope	Constant	R^2	Compound	Slope	Constant	R^2
	C18:0	1.728	43.7	0.645	C20:3 n6	-0.175	0.715	0.616
	PUFA	-3.6	21.3	0.725				
Liver PE	**5 days**				**10 days**			
	Compound	Slope	Constant	R^2	Compound	Slope	Constant	R^2
					Σn3	2.23	6.66	0.617

ACL, average chain length; MUFA, total monounsaturation; PC, phosphatidylcholine; PE, phosphatidylethanolamine; PI, phosphatidylinositol; PUFA, total polyunsaturation; UI, unsaturation index; Σn3, total omega-3 fatty acids; Σn6, total omega-6 fatty acids.

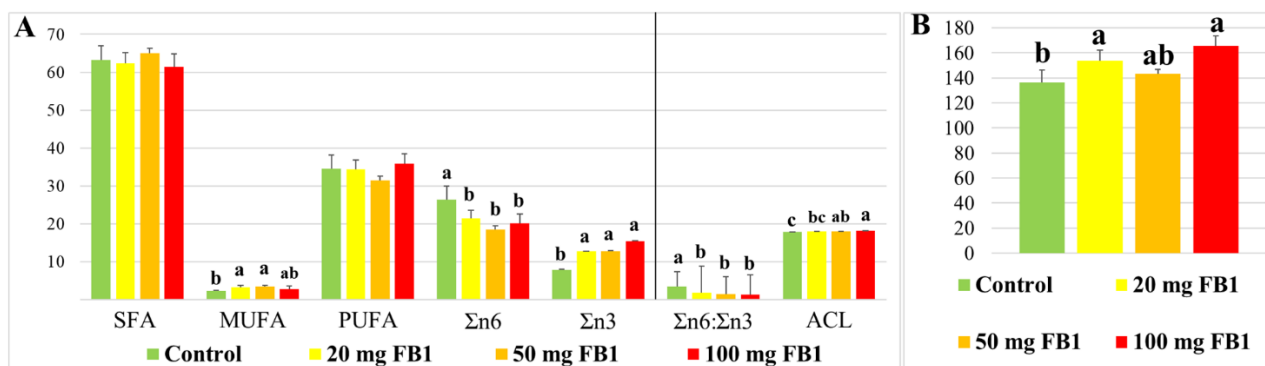### 3.1.2. Calculated indices of fatty acids

The calculated indices of various phospholipids from the kidney and liver corresponded to their significant modifications in fatty acids. In the kidney, both PC and PI showed increases in total saturation and MUFA upon exposure to FB_1, while there were proportional reductions in PUFA and its different fractions ($\Sigma n3$ and $\Sigma n6$). The depletion in PUFA levels had extensive effects, leading to a decrease in UI and ACL (Figures 1 and 2). In the liver, PE displayed some similar patterns, primarily in MUFA and $\Sigma n6$; however, the $\Sigma n3$ levels were increased in rats gavaged with FB_1. Despite the depletion of $\Sigma n6$ in liver PE, the increase in $\Sigma n3$ led to an increase in UI and ACL (Figure 3).
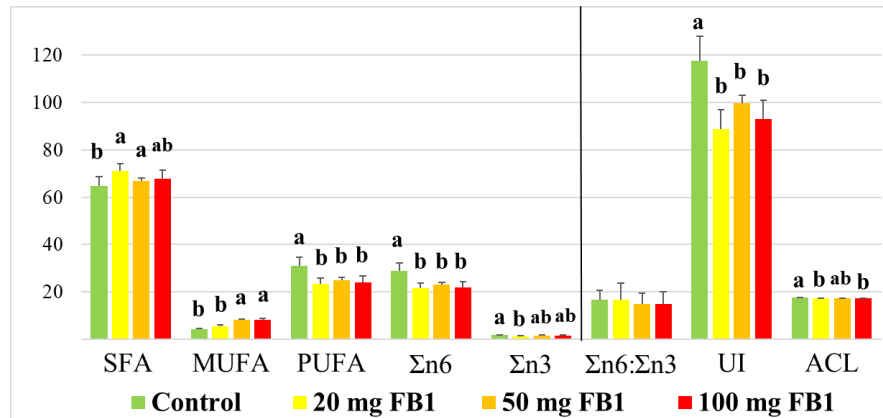
Figure 1. Calculated indices of fatty acids from the renal phosphatidylcholine fraction after 10 days of exposure to different levels of FB_1. The letters (a and b) above the bars indicate the presence of significance at a p-value < 0.05. The columns represent means, while the bar lines represent standard deviations. Abbreviations: ACL, average chain length; MUFA, total monounsaturation; PUFA, total polyunsaturation; SFA, total saturation; UI, unsaturation index; $\Sigma n3$, total omega-3 fatty acids; $\Sigma n6$, total omega-6 fatty acids.
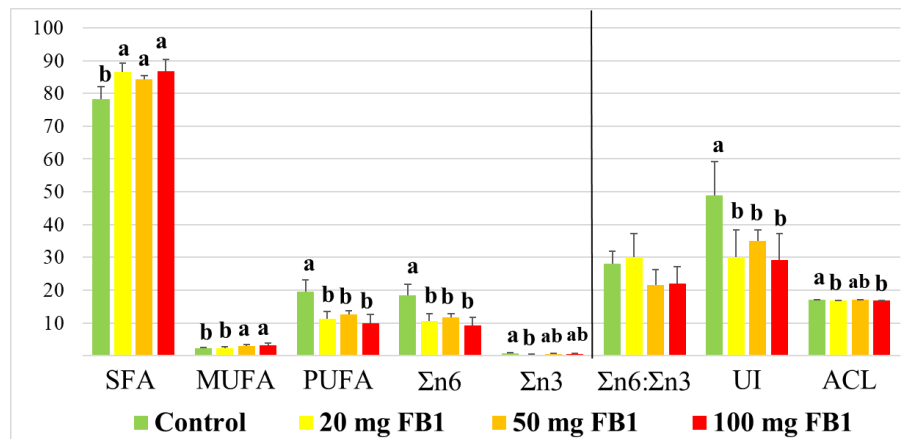
Figure 2. Calculated indices of fatty acids from the renal phosphatidylinositol fraction after 10 days of exposure to different levels of FB_1. The letters (a and b) above the bars indicate the presence of significance at a p-value < 0.05. The columns represent means, while the bar lines represent standard deviations. Abbreviations: ACL, average chain length; MUFA, total monounsaturation; PUFA, total polyunsaturation; SFA, total saturation; UI, unsaturation index; $\Sigma n3$, total omega-3 fatty acids; $\Sigma n6$, total omega-6 fatty acids.

12

Figure 3. Calculated indices of fatty acids from the hepatic PE fraction after 10 days of exposure to different levels of FB_1. A) Columns represent the data of SFA, MUFA, PUFA, Σn6, Σn3, Σn6: Σn3, and ACL. B) Columns represent the data of the UI. The small letters (a, b, and c) above the columns indicate the presence of significance at a p-value < 0.05. The columns represent means, while the bar lines represent standard deviations. Abbreviations: ACL, average chain length; MUFA, total monounsaturation; PUFA, total polyunsaturation; SFA, total saturation; UI, unsaturation index; Σn3, total omega-3 fatty acids; Σn6, total omega-6 fatty acids.

3.2. Orally administered fumonisins affect porcine red cell membrane sodium pump activity and lipid profile without apparent oxidative damage

### 3.2.1. Red cell membrane sodium pump activity and dose response

After 3 weeks of FBs-feeding, there was a difference between the control and the 30 mg FB_{1+2+3}/kg groups in the red cell membrane sodium pump activity (Figure 4). The FBs feeding increased the sodium pump activity significantly only in the latter group, while the 15 mg FB_{1+2+3}/kg treatment provided intermediate data (control $< 15 < 30$) but without statistical significance. Testing the dose response of this alteration, the linear estimation was significant (y intercept $= 52,982$; slope $= 35,340$; sig.: 0.036; $R^2 = 0.58$).
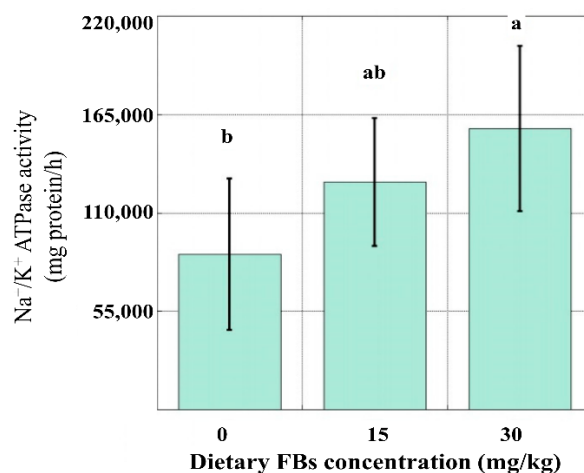
Figure 4. The total Na^+/K^+ ATPase activity of red cells in the experimental piglet groups. The small letters (a and b) above the bars indicate the presence of significance at a p-value < 0.05.

13

3.2.2. Red cell fatty acid profile and dose-response

The fatty acid profile did not provide clear patterns among trial groups (*data shown partially, whereas full data is available in the long version of the thesis*). For example, the control group had the highest proportion of C12:0 (lauric acid), while the 15 mg/kg treatment had the lowest, with the 30 mg/kg treatment showing intermediate values. Clear toxin dose-dependent differences were found for oleic acid, C20:3 DGLA, AA, and MUFA, with the 15 mg/kg group showing higher values than the 30 mg/kg treatment. In all these instances, the control group had intermediate proportional values. The only compound for which the 15 mg/kg group had the lowest proportion was C16:0 (palmitic acid), and as a direct consequence, the sum of saturated fatty acids (Figure 5). As a consequence of this non-linear alteration mode, a well-fitting linear dose-response was not proven in any of the cases.
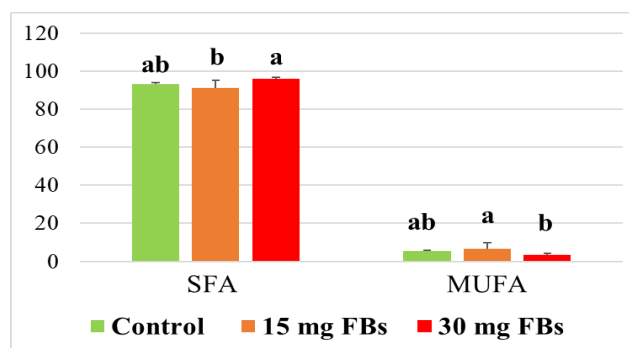
Figure 5. Calculated indices of fatty acids from red cell membranes after 21 days of exposure to different levels of FBs. The small letters (a, b, and c) above the columns indicate the presence of significance at a *p*-value < 0.05. The columns represent means, while the bar lines represent standard deviations. Abbreviations: MUFA, total monounsaturation; SFA, total saturation.

3.2.3. Sodium pump activity correlations

The Pearson correlation between the membrane fatty acid proportions and the sodium pump activity values is given in Table 2, for a description of the inter-relationship between the variables. Practically all individual n6 FAs provided negative correlation with the sodium pump activity as well as the PUFA.

Table 2. Pearson correlation parameters between sodium pump activity and the fatty acid profile data. Significance was set to *p*-value ≤ 0.05).

Compound	*p*-value	Pearson Corr. Coeff.
C18:2 n6	0.017	−0.671
C20:2 n6	0.001	−0.821
C20:3 n6	0.022	−0.65
C20:4 n6	0.023	−0.648
PUFA	0.012	−0.697
Σn6	0.014	−0.683

PUFA, total polyunsaturation; Σn6, total omega-6 fatty acids.

14

3.2.4. Red cell antioxidant status and lipid peroxidation

Whole red cell homogenate reduced glutathione (GSH), glutathione peroxidase (GSHPx), conjugated diene and triene concentrations (CD and CT), and MDA concentration did not provide any inter-group differences (*data is available in the long version of the thesis*), neither linear dose-response, nor any correlations with the sodium pump activity.

3.3. Fumonisin B series mycotoxins' dose dependent effects on the porcine hepatic and pulmonary phospholipidome

### 3.3.1. Animal growth performance

None of the offered doses (15 and 30 mg/kg diet) of FBs was able to induce a remarkable modification in the animals' final body weight or gain, absolute and relative liver and lung weights, feed intake, or feed conversion efficiency (*data is available in the long version of the thesis*).

3.3.2. Dose-response relationship of fatty acids to fumonisins

Analysis of membrane lipid fractions, including sphingomyelins, PCs, PEs, phosphatidylserines (PS), and PIs, in porcine liver and lungs revealed variations in their profiles (Figures 6 and 7). Across these phospholipid fractions, fatty acids of PC and PS were the most responsive to FBs (Table 3). The fatty acid composition of PC, in both liver and lungs, showed dose responses to fed-FBs levels. In the liver, proportions of fatty acids (C16:1 n7 and oleic acid) and MUFA increased proportionally, while in the lungs, DHA, Σn3, and Σn6:Σn3 decreased. In addition, the lung exhibited a dose response in another phospholipid fraction, the PS, where C22:0 and C24:0 decreased with increasing FBs doses.
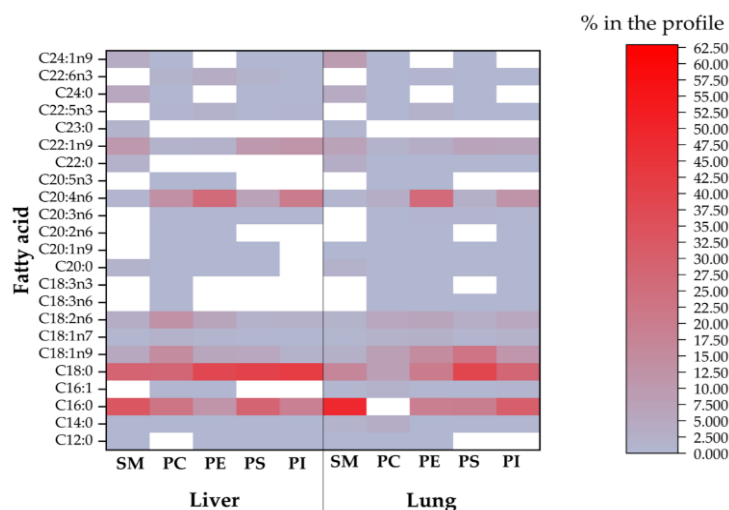
Figure 6. The compositional data of the FAs of all phospholipids from the investigated livers and lungs (SM = sphingomyelin; PC = phosphatidylcholine; PE = phosphatidylethanolamine; PS = phosphatidylserine; PI = phosphatidylinositol). The FA proportion increases with color intensity, whereas the white color represents FA methyl esters below the detection limit of the GC.

15
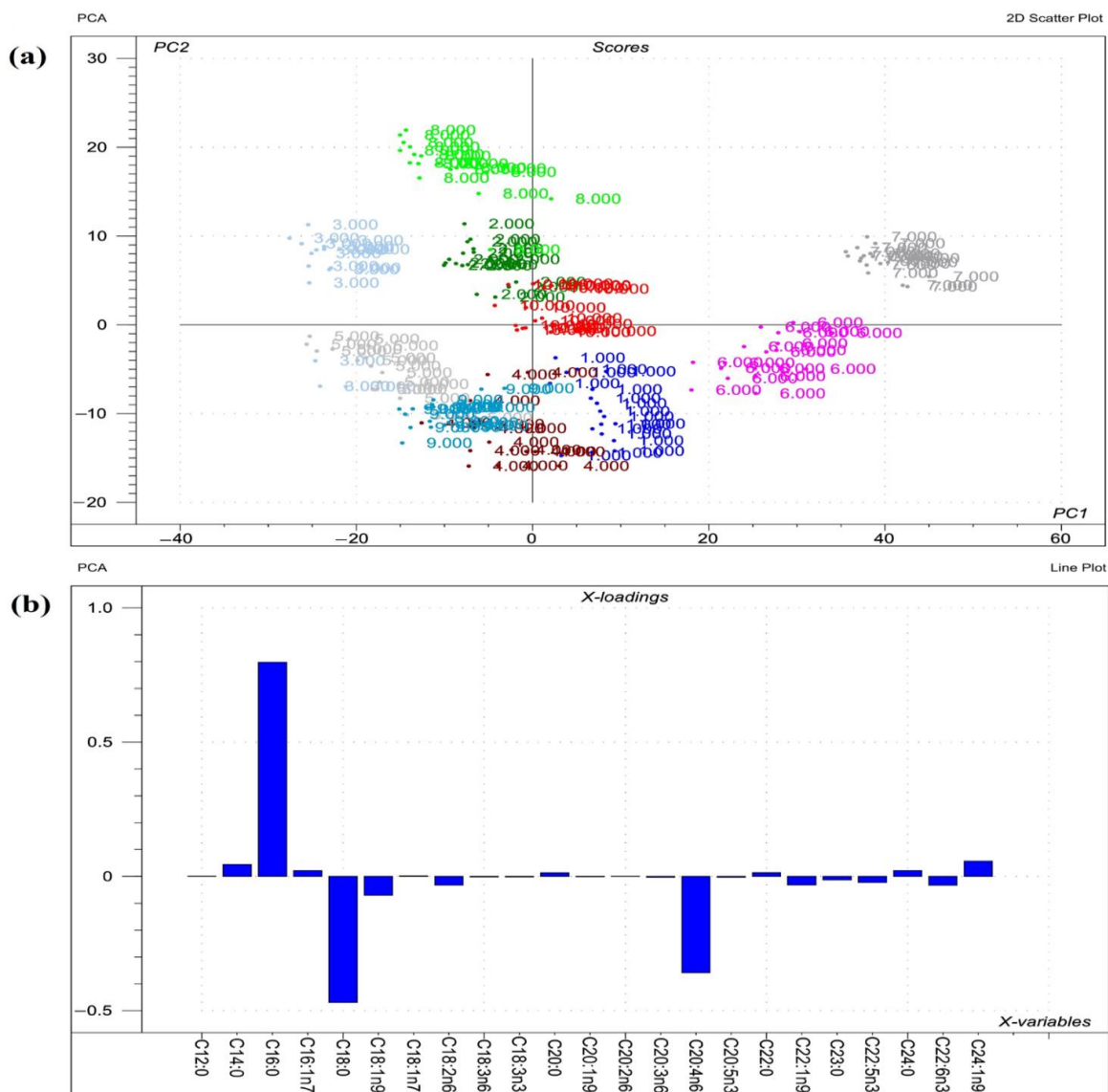
Figure 7. Results of the principal component analysis (PCA) performed on the raw compositional data of the fatty acids of phospholipids from organs. (a) The score plot depicts the orientation of the phospholipid classes from various organs (1 = liver sphingomyelin; 2 = liver phosphatidylcholine; 3 = liver phosphatidylethanolamine; 4 = liver phosphatidylserine; 5 = liver phosphatidylinositol; 6 = lung sphingomyelin; 7 = lung phosphatidylcholine; 8 = lung phosphatidylethanolamine; 9 = lung phosphatidylserine; 10 = lung phosphatidylinositol) in the plane of the first and second principal components (PC1 and PC2, respectively), where PC1 and PC2 are influenced by the multivariate data of fatty acid of the organ phospholipids. PC1 and PC2 explain 64% and 17% of the total variance of the membrane FAs of the phospholipids, respectively. From the PCA, the polar fatty acid pool of phospholipids from liver and lungs provided a perfect spatial separation of groups, referring to variation in their FA profiles; (b) The loading bar graph of the PC1 shows the contribution of the individual fatty acids from tissues to the newly developed latent variable; the higher the loading value, the greater is the impact of the respective fatty acid's variance on the variance of PC1. From the loadings, the remarkable FAs that contributed to the variance between organs are C16:0, C18:0, C20:4n6, C18:1n9, and C24:1n9.

16

Table 3. Phospholipid fractions and their fatty acids that provided linear dose response. Data represent only cases with R^2 above 0.6.

Liver				Lung			
Parameter	**Slope**	**Constant**	$\mathbf{R^2}$	**Parameter**	**Slope**	**Constant**	$\mathbf{R^2}$
Phosphatidylcholine				**Phosphatidylcholine**			
C16:1 n7	89.188	−44.129	0.69	C22:6 n3	−178.028	31.164	0.705
C18:1 n9	4.073	−44.357	0.633	Σn3	−133.946	53.773	0.667
MUFA	3.71	−53.704	0.609	Σn6:Σn3	1.027	−20.943	0.594
				Phosphatidylserine			
				C22:0	−52.0917	40.488	0.782
				C24:0	−134.894	40.566	0.645

MUFA, total monounsaturation; Σn3, total omega-3 fatty acids; Σn6, total omega-6 fatty acids

3.3.3. Calculated indices of fatty acids in phosphatidylcholines

The calculated indices of phosphatidylcholine were consistent with the findings observed in the dose response (Figure 8). Primarily in the porcine liver, MUFA levels increased to compromise levels of PUFA and its respective classes (Σn6 and Σn3), resembling the findings observed in rat liver PCs. In the lung, systematic patterns (decreased) were only noticed in Σn3, which resulted in high Σn6:Σn3.
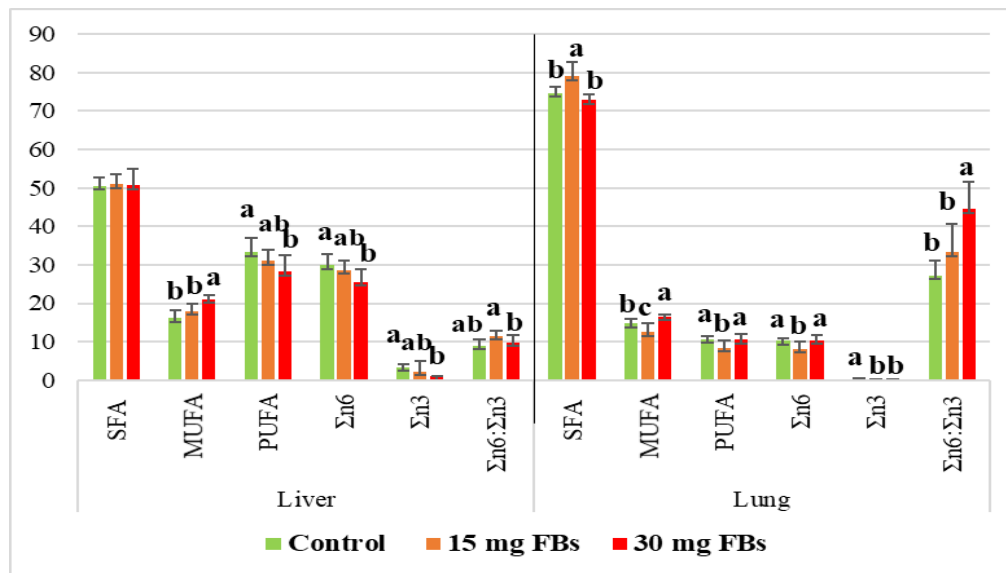

Figure 8. Calculated indices of fatty acids from liver and lung PC fractions after 21 days of exposure. The small letters (a and b) above the bars indicate the presence of significance at a p-value < 0.05. The columns represent means, while the bar lines represent standard deviations.

3.3.4. Antioxidants and lipid peroxidation

Regardless of the FBs dose applied and the investigated organ, no intergroup difference was detected in any of the investigated antioxidant parameters (GSH content and GSHPx activity) or in MDA (*data is available in the long version of the thesis*).

3.3.5. Pathological assessment

During the study, mortality did not occur. Based on necropsy data, only one animal in the 30 mg FBs/kg group showed pale liver. In the lungs, slight vasodilatation and hyperaemia in the mesenterium were observed in some piglets from control and FBs-treated animals. The histological assessment, expressed as a total lesion score, of the liver and lungs is shown in Figure 9. In the liver, the total-lesion score responded positively to the applied FBs level, expressing low cellular glycogen, hepatocyte necrosis, as well as swelling and proliferation of the mononuclear phagocyte system (MPS). Furthermore, the liver provided a dose-dependent response, in which 15 and 30 mg FBs/kg diet expressed mild and moderate intoxication, respectively. Despite the fact that lesions were found in the lungs (Figure 9a), no marked differences were found in the total lesion score among the groups (the detected total scores were not above the mild toxicity level). The PPE was only recorded in a piglet fed on a 30 mg FBs/kg diet, in which the lung was expressed as heavy, swollen, pale, and doughy.
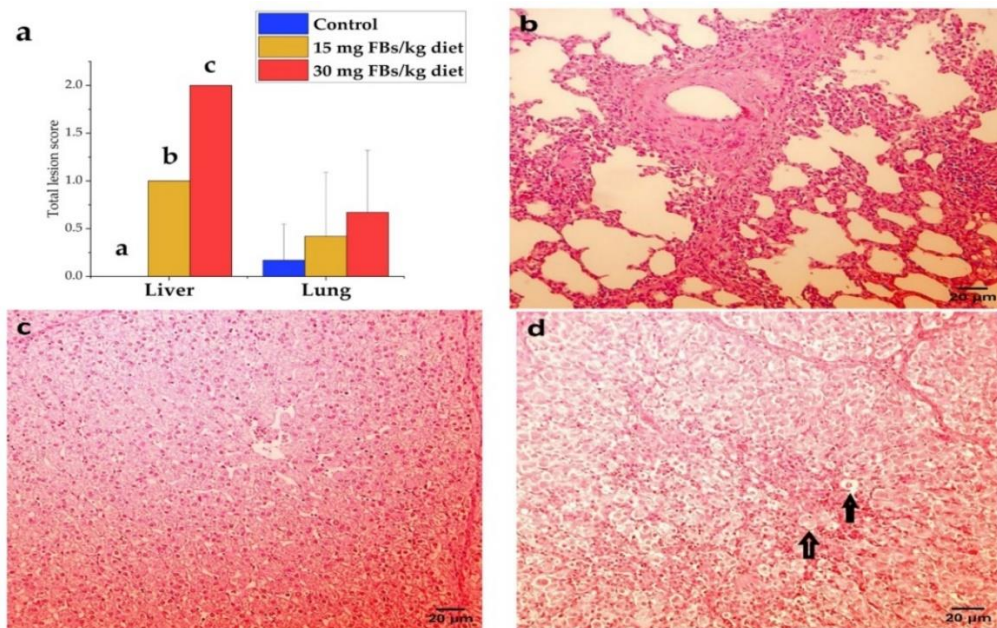

Figure 9. (a) Total lesion scores of livers and lungs recorded in experimental piglets (n = 6 animals/treatment, whereas columns represent means, and bars represent the standard deviation. The letters a, b, and c above the bars indicates significant differences). (b) Lung of a healthy pig with mild lymphocytic and histiocytic infiltration in connective tissue (hematoxylin–eosin, 200 ×, scale bar = 20 μm). (c) A healthy piglet liver from control, where the cytoplasm of hepatocytes is finely granulated due to high glycogen content, resulting in an intense stain (hematoxylin–eosin, 200 ×, scale bar = 20 μm), although a PAS stain would be necessary to confirm our observation. (d) The liver of a highly FBs intoxicated piglet (30 mg/kg), where the glycogen content decreased in the hepatocytes' cytoplasm and a high frequency of necrotic (rounded, faintly stained) hepatocytes (↑) detected (hematoxylin–eosin, 200 ×, scale bar = 20 μm).

3.4. A 65-day fumonisin B exposure at high dietary levels has negligible effects on the testicular and spermatological parameters of adult rabbit bucks

3.4.1. Animal performance

The initial and final body weights displayed no marked differences across groups. As shown in Figure 10, the graded FB levels likewise lowered group mean body weight, in a systematic manner, but without statistical significance. The feed intake was measured daily until day 25, then weekly, but provided no inter-group differences (*data is available in the long version of the thesis*).
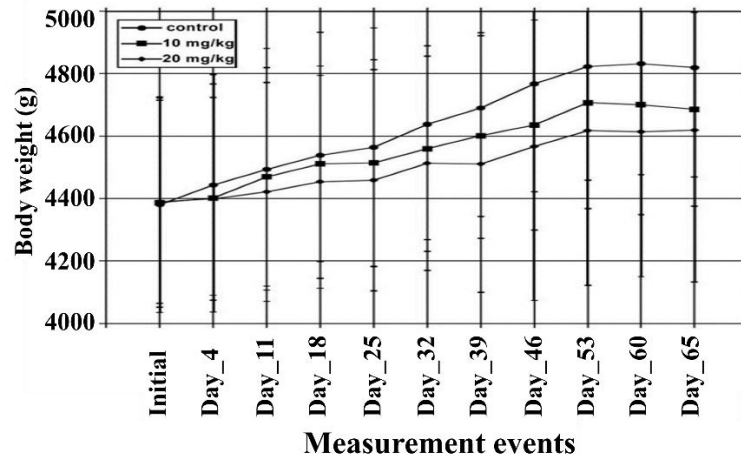

Figure 10. Body weight changes along the study period of the three rabbit groups (n = 10 animals/treatment).

3.4.2. Spermium morphology, chromatin integrity, distribution and viability

The flow cytometric live and dead cellular distribution pattern is shown in Figure 11A in a representative sample, providing a very effective separation. Debris events were excluded from the analysis. When analyzing the live cell proportion within the total cell counts, no systematic difference could be established (*data is available in the long version of the thesis*); differences were not significant even at p-value < 0.05 if analyzing the five consecutive samplings within the single groups and even if the three experimental groups were compared with each other at the five sampling events. Live/dead spermatozoa ratio at the ultimate sampling was 84.3 ± 2.95, 75.8 ± 7.36 and 74.4 ± 21.8, for the control, 10 and 20 mg FB_{1+2+3}/kg treatments, respectively.

On Feulgen-stained semen smears, abnormal spermatozoa and disturbances in chromatin condensation were recorded with light microscopic counting. Figure 11B provides typical demonstrations of some of the most frequent cellular defects observed. Morphological abnormalities were classified as head or tail defects; neither of these showed a significant difference over time or between treatments (*data is available in the long version of the thesis*).

19
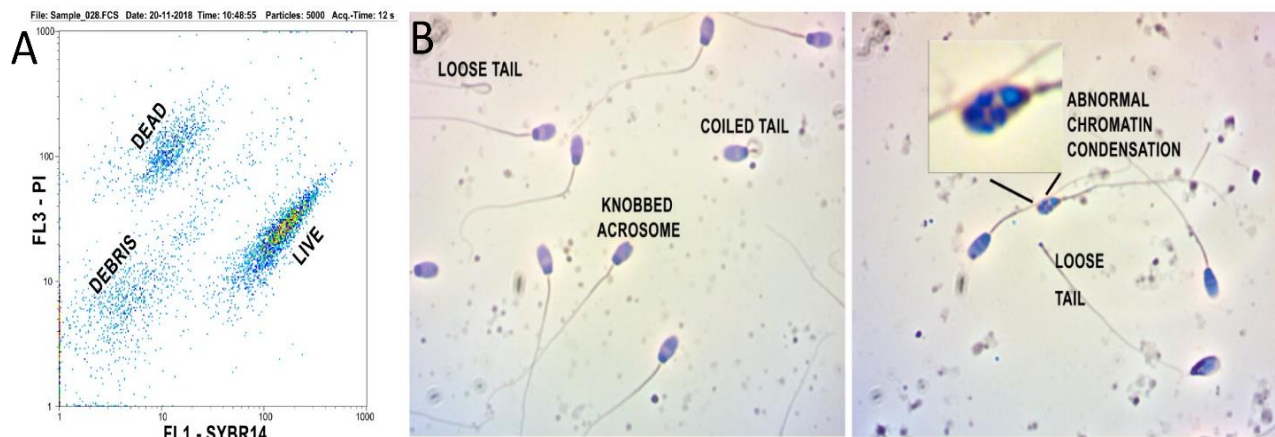
Figure 11. A) Flow cytometric dot-plot showing the green (SYBR14) and red (PI) fluorescence properties of live and dead spermatozoa; the lower left population was identified as debris and was excluded from data analysis. B) Abnormal morphology of the rabbit spermatozoa. (Feulgen staining, 400× magnification). Inner photo: abnormally condensed chromatin showing a patchy staining pattern.

3.4.3. Spermium membrane fatty acid composition

We only determined the control vs. the two intoxicated cases at the last sampling event, and since there was absolutely no systematic inter-group difference detectable, further, retrospective analysis was avoided (*data is available in the long version of the thesis*).

3.4.4. Testicular Phospholipid Fatty Acid Composition

When comparing the group means, there was a detectable difference only in the proportion of C17:0, margaric acid (increased in the 20 mg FBs/kg group, *p*-value = 0.002 for the ANOVA model). Any other individual fatty acids or calculated variables failed to provide inter-group differences (*data is available in the long version of the thesis*).

3.4.5. Testicular lipid peroxidation and antioxidants

The results of the testicular antioxidant and lipid peroxidation parameters are shown in Table 4. FBs feeding significantly increased the concentration and activity of reduced glutathione (GSH) and glutathione peroxidase (GSHPx), in both intoxicated groups, as compared to the control, in a dose dependent manner (Figure 12). Initial phase lipid peroxidation decreased slightly (CD and CT, i.e., conjugated dienes and trienes) with the increasing FBs' levels, while end-phase lipid peroxidation (MDA) was not proven.

Table 4. Testicular antioxidant and lipid peroxidation parameters in the three experimental rabbit groups.

| Group	Control Mean	±	SD	10 mg/kg Mean	±	SD	20 mg/kg Mean	±	SD
GSH (µmol/g prot.)	6.57	±	0.55 b	7.54	±	0.7 a	7.9	±	0.98 a
GSHPx (IU/g prot.)	6.25	±	0.66 b	7.45	±	0.85 a	7.5	±	0.65 a
MDA (nmol/g)	44.7	±	9.11	39	±	7.17	38.5	±	7.22
CD (Abs. 232 nm)	0.34	±	0.02 a	0.34	±	0.03 a	0.31	±	0.02 b
CT (Abs. 268 nm)	0.16	±	0.01 a	0.15	±	0.01 ab	0.14	±	0.01 b

GSH, reduced glutathione; GSHPx, glutathione peroxidase; MDA, malondialdehyde; CD, conjugated dienes; CT, conjugated trienes, U, unit, A: absorbance
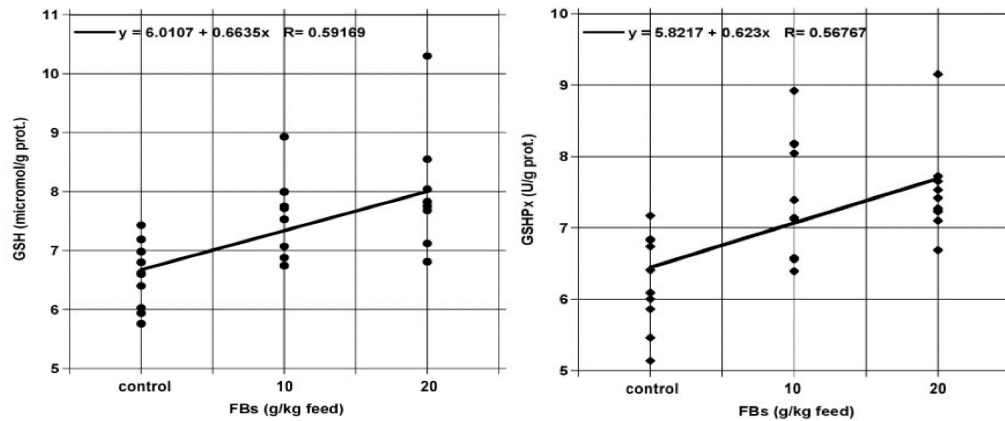
Figure 12. Linear dose-dependence for GSH (●) and GSHPx (♦) in the rabbit testis.

3.4.6. Testis histology

The testicular tissue sections were evaluated in all animals and provided no group-dependent differences. A typical section pair is shown in Figure 13a,b.
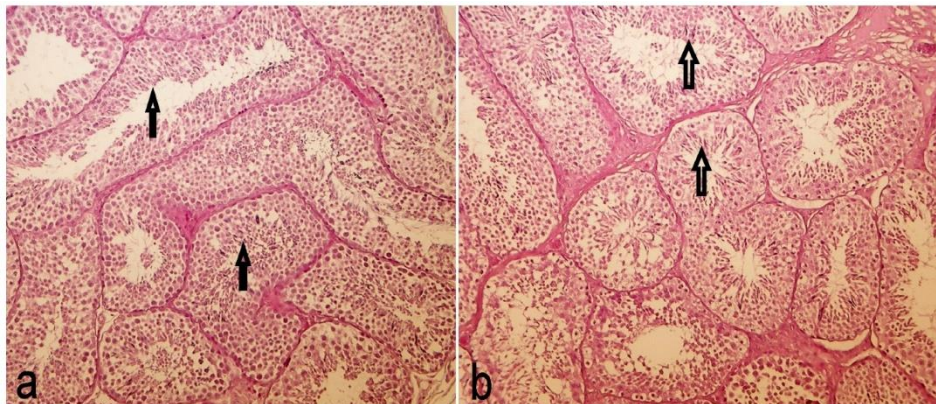
Figure 13. Testis histology of a control (a) and an intoxicated (b; 20 mg/kg FBs, 65 days exposure) rabbit buck (hematoxylin-eosin staining, 200× magnification).

4. CONCLUSIONS AND RECOMMENDATIONS

The initial study revealed that the rat kidney was highly reactive, showing modifications in the membrane fatty acid compositions of different phospholipid fractions due to low dosage and short-term exposure to FB_1. The most responsive phospholipid fraction in the rat renal cortex was PC, which displayed fatty acid proportional shifts in $\Sigma n6$, $\Sigma n3$, and consequently, $\Sigma PUFA$ (dose-dependent decreases), while $\Sigma MUFA$ showed a dose-response increase. This dose-dependent pattern was somewhat partial and present in PIs, particularly in $\Sigma PUFA$. The rat liver demonstrated less sensitivity to FB_1, with the PE fraction revealing a dose-response relationship. These results align with previously published histopathological and peroxidation endpoint findings (Szabó *et al.*, 2018). In respect to this, alterations in membrane fatty acids could potentially be used to determine the extent of histological sensitivity. Although the role of lipid peroxidation in depleting PUFAs has been acknowledged, indices relating to enzymes involved in lipid metabolism suggest possible alterations in enzyme activity. Therefore, further investigation of phospholipid-metabolizing enzymes is important for understanding the potential impact of enzyme perturbation on cellular membrane remodeling.

In species other than rabbits, specifically swine (weaned piglets), the activity of the sodium-potassium pump was assessed during the second study. The diet contained FBs at levels of 15 and 30 mg/kg, which notably altered the Na^+/K^+ ATPase activity of erythrocytes after a period of three weeks, showing a dose-dependent increase. This observation suggests that erythrocyte damage or functional changes are a feature of FBs and are not limited to rabbits. The substantial increase in sodium pump activity is most likely triggered by FB_1's inhibitory effect on CerS. This particular mycotoxin induces a state associated with nonoxidative stress, characterized by a marked increase in sodium pump activity and a complex fatty acid profile of membrane lipids, offering pertinent correlations for all n-6 fatty acids. It is postulated that additional research is required to elucidate the role of cellular lipids in the proven regulatory function of Na^+/K^+ ATPase. It is highly likely that these studies will need to segregate lipid classes into more relevant subclasses prior to conducting fatty acid analysis.

In a relatively, partially, similar approach to the first study, the third investigation assessed the impact of FBs on the fatty acid profiles of membrane lipids in piglets' livers and lungs, with the effects observed to be dose-dependent. This is the first study to document modifications in the fatty acid profiles of phospholipid classes in the livers and lungs of piglets following exposure to FBs. The relatively high dosage of FBs did not have a marked effect on piglet production traits or oxidative stress markers. Only subtle, characteristic effects were identified in the fatty acid profiles of membrane

lipid fractions. Dose-dependent linear alterations were noted in liver PC as well as in lung PC and PS fractions. The data collected revealed variations in tissue-specific responses in membrane lipids. Additionally, the findings indicate a distortion in the activities of enzymes related to fatty acid metabolism, such as elongase, D5D, D6D, and Δ9D. These enzyme alterations were characterized by a proportional decrease in PUFAs and an increase in ΣMUFA. The changes observed in membrane lipids are not primarily considered to be responsible for liver and lung toxicity but rather are consequences or mediators of other events that may have led to tissue damage. This study did not include the quantitative determination of ceramide and polar lipids, which could offer further insight into the findings. Therefore, additional studies investigating the quantitative effects of FBs on the lipidomes of the liver and lungs are highly important.

Since the toxicity potential of FBs to the reproductive systems of animals, such as rabbits and swine, has been reported, the third study assessed the effects of FBs on adult male rabbit bucks. Exposure to FBs over an entire testicular cycle did not result in substantial modifications at five sampling points in the spermatozoa endpoints (proportion of live cells, morphological distribution, membrane lipid profile). However, a slight increase in antioxidant defense was observed in the testes without any striking alterations in the lipid profile or histological modifications. However, a minimal pro-oxidant effect of FBs on the male genital system was observed, with no marked detrimental impact on the examined spermatological traits. Thus, the reproductive system of adult male bucks appears to be resistant to the applied mycotoxins over a period of 65 days. Apparently, additional studies involving a longer exposure period and the inclusion of growing rabbits would provide further understanding of potential response variations.

5. NEW SCIENTIFIC RESULTS

The scientific outcomes presented herein are derived from four distinct studies conducted during the course of this doctoral research.

1. Observations from the rat study indicate that alterations in the fatty acid composition of hepatocellular membranes may likely occur at lower fumonisin B1 (FB_1) exposure levels ($<$ 50 mg FB_1/kg^{-1} dietary dose equivalent for 5 days) compared to the high doses (150 and 250 mg/kg diet for a period over 21 days) reported in earlier studies.

2. Fatty acid alterations induced by FB_1 in rat kidneys were the most prevalent (especially at 100 mg FB_1/kg^{-1} dietary dose equivalent for 10 days), providing a negative dose-response for polyunsaturated fatty acids, and a positive dose-response for saturated fatty acids and monounsaturated fatty acids (MUFAs) of phosphatidylcholines (PC) and phosphatidylinositols (PI). In contrast, liver phosphatidylethanolamine was the only phospholipid fraction that exhibited a positive dose-response for the sum of omega-3 fatty acids ($\Sigma n3$).

3. The modulation of ion exchange pump, Na^+/K^+ ATPase activity, by FB_{1+2+3} (FBs) in porcine erythrocytes was proven, a phenomenon previously not deliberately investigated in any species other than rabbits.

4. An increase in erythrocyte Na^+/K^+ ATPase activity was observed in a dose-dependent manner following the administration of FBs (15 and 30 mg/kg feed for 21 days) for the first time, at least in the studied animal model (pig) and its age. Furthermore, the findings indicated a negative correlation ($r > -0.6$) between the activities of Na^+/K^+ ATPase and omega-6 (n6) fatty acids, including linoleic, eicosadienoic, dihomo-γ-linolenic and arachidonic acids.

5. Similar to rats, piglets exposed to FBs (15 and 30 mg/kg diet for 21 days) exhibited altered fatty acid compositions of various phospholipid fractions, especially PC, phosphatidylethanolamine, and phosphatidylserine (PS), in the lungs and livers.

6. In piglets, dose-dependent responses were observed between the administered doses of FBs (15 and 30 mg/kg feed) and fatty acids (C16:1 n7, C18:1 n9, and sum of MUFAs (ΣMUFA)) in liver PCs, as well as in pulmonary PCs (C22:6 n3, $\Sigma n3$, and $\Sigma n6:\Sigma n3$) and PSs (C20:0, and C24:0).

7. Based on the findings in piglets, oxidative stress (as assessed by malondialdehyde) does not appear to be directly involved in FBs toxicity, suggesting that fatty acid modifications and

histological lesions may occur independently of oxidative stress and involve other events, such as disruption of lipid metabolism and membrane remodeling enzymes.

8. Adult male rabbits appear to be resistant to doses (10 and 20 mg/kg diet) of FBs above the EU-permitted levels for over 65 days, as these mycotoxins did not compromise body weight or feed efficiency, or alter the membrane lipids of their reproductive system.

6. REFERENCES

Barth, A. D., & Oko, R. J. (1989). Abnormal Morphology of Bovine Spermatozoa; *Ames, Iowa State University Press: Ames*, IA, USA. viii + 285pp. available at: https://www.cabidigitallibrary.org/doi/full/10.5555/19900178378

Bedin, M., Helena, C., Estrella, G., Ponzi, D., Duarte, D.V., Dutra-Filho, C.S., Wyse, A. T. S., Wajner, M., & Wannmacher, C. M. D. (2001). Reduced Na+,K+-ATPase activity in erythrocyte membranes from patients with phenylketonuria. *Pediatric Research, 50*, 56–60. https://doi.org/10.1203/00006450-200107000-00012

Bennett, J. W., & Klich, M. (2003). Mycotoxins. *Clinical Microbiology Reviews*, *16*(3), 497–516. https://doi.org/10.1128/CMR.16.3.497-516.2003

Bills, G. F., & Gloer, J. B. (2016). Biologically Active Secondary Metabolites from the Fungi. *Microbiology Spectrum*, *4*(6). https://doi.org/10.1128/microbiolspec.FUNK-0009-2016

Bełtowski, J., & Wójcicka, G. (2002). Spectrophotometric method for the determination of renal ouabain-sensitive H+,K+-ATPase activity. *Acta Biochimica Polonica*, *49*(2), 515–527. Available at: https://bibliotekanauki.pl/articles/1043791

Burger, H.-M., Abel, S., & Gelderblom, W. C. A. (2018). Modulation of key lipid raft constituents in primary rat hepatocytes by fumonisin B1 - Implications for cancer promotion in the liver. *Food and Chemical Toxicology*, *115*, 34–41. https://doi.org/10.1016/j.fct.2018.03.004

Christie, W.W. (1982). A simple procedure for rapid transmethylation of glycerolipids and cholesteryl esters. *Journal of Lipid Research, 23*(7), 1072–1075. https://doi.org/10.1016/S0022-2275(20)38081-0

Christie W.W. (2003). Lipid analysis: isolation, separation, identification, and structural analysis of lipids. Dundee, Scotland: *Oily Press*.

Djemli-Shipkolye, A., Raccah, D., Pieroni, G., Vague, P., Coste, T.C., & Gerbi, A. (2003). Differential effect of ω3 PUFA supplementations on Na,K-ATPase and Mg-ATPase activities: Possible role of the membrane ω6/ω3 ratio. *Journal of Membrane Biology, 191*, 37–47. https://doi.org/10.1007/s00232-002-1039-z

dsm-firmenich. (2023). World mycotoxin survey: the global threat January – December 2023. https://www.dsm.com/content/dam/dsm/anh/en/documents/REP_MTXsurvey_Q4_2023_EN_0124_AUE_doublePage.pdf

El-Sayed, R. A., Jebur, A. B., Kang, W., & El-Demerdash, F. M. (2022). An overview on the major mycotoxins in food products: characteristics, toxicity, and analysis. *Journal of Future Foods*, *2*(2), 91–102. https://doi.org/10.1016/j.jfutfo.2022.03.002

Fliszár-Nyúl, E., Faisal, Z., Skaper, R., Lemli, B., Bayartsetseg, B., Hetényi, C., Gömbös, P., Szabó, A., & Poór, M. (2022). Interaction of the Emerging Mycotoxins Beauvericin, Cyclopiazonic

Acid, and Sterigmatocystin with Human Serum Albumin. *Biomolecules, 12*(8), 1106. https://doi.org/10.3390/biom12081106

Fodor, J., Kametler, L., & Kovács, M. (2006). Practical aspects of fumonisin production under laboratory conditions. *Mycotoxin Research, 22*(4), 211–216. https://doi.org/10.1007/bf02946744

Folch, J., Lees, M., & Stanley, G. H. S. (1957). A simple method for the isolation and purification of total lipides from animal tissues. *Journal of Biological Chemistry*, *226*(1), 497–509. https://doi.org/10.1016/S0021-9258(18)64849-5

Heape, A. M., Juguelin, H., Boiron, F., & Cassagne, C. (1985). Improved one-dimensional thin-layer chromatographic technique for polar lipids. *Journal of Chromatography A*, *322*, 391–395. https://doi.org/10.1016/S0021-9673(01)97702-7

Hurst, R. O. (1964). The determination of nucleotide phosphorus with stannous chloride-hydrazine sulphate reagent. *Canadian Journal of Biochemistry*, *42*(2), 287–292. https://doi.org/10.1139/o64-033

Leray, C., Pelletier, X., Hemmendinger, S., & Cazenave, J.P. (1987). Thin-layer chromatography of human platelet phospholipids with fatty acid analysis. *J. Chromatogr. B Biomed. Sci. Appl., 420*, 411–416. https://doi.org/10.1016/0378-4347(87)80198-6

Lowry, O. H., Rosebrough, N. J., Farr, A. L., & Randall, R. J. (1951). Protein measurement with the Folin phenol reagent. *Journal of Biological Chemistry*, 1951, *193*(1), 265–275. https://doi.org/10.1016/S0021-9258(19)52451-6

Matkovics, B., Szabó, L., & Varga, S. (1988). Determination of lipid peroxidation and reduced glutathione metabolism enzymes activities in biological samples. *Laboratóriumi Diagnosztika, 15*, 248–250.

Nagy, S., Jansen, J., Topper, E. K., & Gadella, B. M. (2003). A triple-stain flow cytometric method to assess plasma- and acrosome-membrane integrity of cryopreserved bovine sperm immediately after thawing in presence of egg-yolk particles. *Biology of reproduction*, *68*(5), 1828–1835. https://doi.org/10.1095/biolreprod.102.011445

OECD Environmental Health and Safety Publications. OECD Principles of Good Laboratory Practice (as Revised in 1997). 1997. Available at: https//ntp.niehs.nih.gov/iccvam/suppdocs/feddocs/oecd/oecd_glpcm.pdf

Pandey, A. K., Samota, M. K., Kumar, A., Silva, A. S., & Dubey, N. K. (2023). Fungal mycotoxins in food commodities: present status and future concerns. *Frontiers in Sustainable Food Systems*, *7*. https://doi.org/10.3389/fsufs.2023.1162595

Placer, Z. A., Cushman, L. L., & Johnson, B. C. (1966). Estimation of product of lipid peroxidation (malonyl dialdehyde) in biochemical systems. *Analytical Biochemistry*, *16*(2), 359–364. https://doi.org/10.1016/0003-2697(66)90167-9

Rahman, I., Kode, A., & Biswas, S. K. (2006). Assay for quantitative determination of glutathione and glutathione disulfide levels using enzymatic recycling method. *Nature Protocols*, 1, 3159–3165. https://doi.org/10.1038/nprot.2006.378

Rheeder, J. P., Marasas, W. F. O., & Vismer, H. F. (2002). Production of Fumonisin Analogs by Fusarium Species. *Applied and Environmental Microbiology*, *68*(5), 2101–2105. https://doi.org/10.1128/AEM.68.5.2101-2105.2002

Riley, R. T., & Merrill, A. H. (2019). Ceramide synthase inhibition by fumonisins: a perfect storm of perturbed sphingolipid metabolism, signaling, and disease. *Journal of Lipid Research*, *60*(7), 1183–1189. https://doi.org/10.1194/jlr.S093815

Shanmugasundaram, K. R., Padmavathi, C., Acharya, S., Vidhyalakshmi, N., & Vijayan, V. K. (1992). Exercise-induced cholesterol depletion and Na+,K(+)-ATPase activities in human red cell membrane. *Experimental Physiology, 77*(6), 933–936. https://doi.org/10.1113/expphysiol.1992.sp003663

Shier, W. T. (2000). The fumonisin paradox: A review of research on oral bioavailability of fumonisin B1, a mycotoxin produced by Fusarium moniliforme. *Journal of Toxicology: Toxin Reviews*, *19*(2), 161–187. https://doi.org/10.1081/TXR-100100319

Szabó, A., Szabó-Fodor, J., Kachlek, M., Mézes, M., Balogh, K., Glávits, R., Ali, O., Zeebone, Y., & Kovács, M. (2018). Dose and Exposure Time-Dependent Renal and Hepatic Effects of Intraperitoneally Administered Fumonisin B1 in Rats. *Toxins*, *10*(11), 465. https://doi.org/10.3390/toxins10110465

Voss, K. A., & Riley, R. T. (2013). Fumonisin Toxicity and Mechanism of Action: Overview and Current Perspectives. *Food Safety*, *1*(1), 2013006–2013006. https://doi.org/10.14252/foodsafetyfscj.2013006

7. PUBLICATION AND PRESENTATIONS

7.1. Peer-reviewed papers relevant to the dissertation

7.1.1. **Ali O**, Szabó A. Fumonisin Distorts the Cellular Membrane Lipid Profile: A Mechanistic Insight. *Toxicology*. 2024. Doi: 10.1016/j.tox.2024.153860. **Q1, IF: 4.922.**

7.1.2. **Ali O**, Szabó A. Review of Eukaryote Cellular Membrane Lipid Composition, with Special Attention to the Fatty Acids. *Int J Mol Sci.* 2023;24(21):15693. Doi: 10.3390/ijms242115693. **D1, IF: 6.266**.

7.1.3. **Ali O,** Mézes M, Balogh K, Kovács M, Turbók J, Szabó A. Fumonisin B Series Mycotoxins' Dose Dependent Effects on the Porcine Hepatic and Pulmonary Phospholipidome. *Toxins (Basel).* 2022;14(11):803. Doi: 10.3390/toxins14110803. **Q1, IF: 4.796**.

7.1.4. Szabó A, Nagy S, **Ali O**, Gerencsér Z, Mézes M, Balogh KM, Bartók T, Horváth L, Mouhanna A, Kovács M. A 65-Day Fumonisin B Exposure at High Dietary Levels Has Negligible Effects on the Testicular and Spermatological Parameters of Adult Rabbit Bucks. *Toxins (Basel).* 2021;13(4):237. Doi: 10.3390/toxins13040237. **Q1, IF: 4.796**.

7.1.5. Szabó A, **Ali O,** Lóki K, Balogh K, Mézes M, Bartók T, Horváth L, Kovács M. Orally Administered Fumonisins Affect Porcine Red Cell Membrane Sodium Pump Activity and Lipid Profile Without Apparent Oxidative Damage. *Toxins (Basel).* 2020;12(5):318. Doi: 10.3390/toxins12050318. **Q1, IF: 4.796**.

7.1.6. Szabó A, Fébel H, **Ali O,** Kovács M. Fumonisin B1 induced compositional modifications of the renal and hepatic membrane lipids in rats - dose and exposure time dependence. *Food Addit Contam Part A Chem Anal Control Expo Risk Assess.* 2019;36(11):1722-1739. Doi: 10.1080/19440049.2019.1652772. **Q2, IF: 3.530**.

7.2. Peer-reviewed papers on the subject of the dissertation but not incorporated

7.2.1. **Ali O,** Mézes M, Balogh K, Kovács M, Szabó A. The Effects of Mixed Fusarium Mycotoxins at EU-Permitted Feed Levels on Weaned Piglets' Tissue Lipids. *Toxins (Basel).* 2021;13(7):444. Doi: 10.3390/toxins13070444. **Q1, IF: 4.796**.

7.2.2. **Ali O**, Szabó-Fodor J, Fébel H, Mézes M, Balogh K, Glávits R, Kovács M, Zantomasi A, Szabó A. Porcine Hepatic Response to Fumonisin B1 in a Short Exposure Period: Fatty Acid Profile and Clinical Investigations. *Toxins (Basel).* 2019;11(11):655. Doi: 10.3390/toxins11110655. **Q1, IF: 4.796**.

7.2.3. Szabó A, Szabó-Fodor J, Kachlek M, Mézes M, Balogh K, Glávits R, **Ali O**, Zeebone YY, Kovács M. Dose and Exposure Time-Dependent Renal and Hepatic Effects of Intraperitoneally Administered Fumonisin B$_1$ in Rats. *Toxins (Basel).* 2018; 10(11):465. Doi: 10.3390/toxins10110465. **Q1, IF: 4.796**.

7.2.4. Szabó A, Szabó-Fodor J, Fébel H, Mézes M, Balogh K, Bázár G, Kocsó D, **Ali O**, Kovács M. Individual and Combined Effects of Fumonisin B$_1$, Deoxynivalenol and Zearalenone on the Hepatic and Renal Membrane Lipid Integrity of Rats. *Toxins (Basel).* 2017; 10(1):4. Doi: 10.3390/toxins10010004. **Q1, IF: 4.796**.

7.3. Peer-reviewed papers not relevant to the topic of the dissertation

7.3.1. Kulcsár S, Turbók J, Kövér G, Balogh K, Zándoki E, Gömbös P, **Ali O,** Szabó A, Mézes M. Exposure to a Combination of Fusarium Mycotoxins Leads to Lipid Peroxidation and Influences Antioxidant Defenses, Fatty Acid Composition of Phospholipids, and Renal Histology in Laying Hens. *Toxins.* 2024; 16(5):226. DOI: 10.3390/toxins16050226. **Q1, IF: 4.796**.

7.3.2. Kulcsár S, Turbók J, Kövér G, Balogh K, Zándoki E, Gömbös P, **Ali O,** Szabó A, Mézes M. The Effect of Combined Exposure of Fusarium Mycotoxins on Lipid Peroxidation, Antioxidant Defense, Fatty Acid Profile, and Histopathology in Laying Hens' Liver. *Toxins.* 2024; 16(4):179. DOI: 10.3390/toxins16040179. **Q1, IF: 4.796**.

7.3.3. Gebremichael A, Szabó A, Sándor ZJ, Nagy Z, **Ali O**, Kucska B. Chemical and Physical Properties of African Catfish (Clarias gariepinus) Fillet Following Prolonged Feeding with Insect Meal-Based Diets. *Aquac Nutr.* 2023; 2023:6080387. Doi: 10.1155/2023/6080387. **Q1, IF: 4.218**.

7.3.4. Yakubu HG, **Ali O,** Szabó A, Tóth T, Bazar G. Feeding Mixed Silages of Winter Cereals and Italian Ryegrass Can Modify the Fatty Acid and Odor Profile of Bovine Milk. *Agriculture.* 2023; 13(2):381. DOI: 10.3390/agriculture13020381. **Q2, IF: 3.916**.

7.3.5. Zeebone YY, Bóta B, Halas V, Libisch B, Olasz F, Papp P, Keresztény T, Gerőcs A, **Ali O,** Kovács M, Szabó A. Gut-Faecal Microbial and Health-Marker Response to Dietary Fumonisins in Weaned Pigs. *Toxins (Basel).* 2023;15(5):328. Doi: 10.3390/toxins15050328. **Q1, IF: 4.796**.

7.3.6. Varga-Visi É, Jócsák I, Kozma V, Lóki K, **Ali O**, Szabó A. Effects of Surface Treatment with Thymol on the Lipid Oxidation Processes, Fatty Acid Profile and Color of Sliced Salami

during Refrigerated Storage. *Foods*. 2022;11(23):3917. Doi: 10.3390/foods11233917. **Q1, IF: 5.738**.

7.3.7. Yakubu HG, **Ali O**, Ilyés I, Vigyázó D, Bóta B, Bazar G, Tóth T, Szabó A. Micro-Encapsulated Microalgae Oil Supplementation Has No Systematic Effect on the Odor of Vanilla Shake-Test of an Electronic Nose. *Foods*. 2022;11(21):3452. Doi: 10.3390/foods11213452. **Q1, IF: 5.738**.

7.3.8. **Ali O,** Petrási Z, Donkó T, Fébel H, Mézes M, Szabó A. Muscle fibre membrane lipid composition in musculus *biceps femoris* of pigs reared in indoor or outdoor systems. *Journal of Animal and Feed Sciences*. 2021;30(3):238-247. Doi:10.22358/jafs/139275/2021. **Q2, IF: 1.876**.

7.3.9. Kócsó DJ, **Ali O**, Kovács M, Mézes M, Balogh K, Kachlek ML, Bóta B, Zeebone YY, Szabó A. A preliminary study on changes in heat shock protein 70 levels induced by Fusarium mycotoxins in rats: *in vivo* study. *Mycotoxin Res*. 2021;37(2):141-148. Doi: 10.1007/s12550-021-00425-z. **Q2, IF: 3.612**.

7.4. Peer-reviewed papers published in Hungarian scientific journal

7.4.1. **Ali O.** A Brief Review of the European Directive on 3Rs and Facilitating Animal Experimentation. *ACTA AGRARIA KAPOSVÁRIENSIS*. 2024; 27 (1),

7.5. Abstracts

7.5.1. Oral presentations

7.5.1.1. **Ali O**, Mézes M, Balogh KM, Kovács M, Mouhanna A, Szabó A. Dose-dependent effects of the dietary fumonisin b series on the liver membrane lipids of weaned piglets. 30th International Symposium Animal Science Days, Zadar, Croatia, 21-23 September, 2022.

7.5.1.2. Szabó A, Nagy S, **Ali O**, Gerencsér Z, Mézes M, Kovács M, Effects of Fumonisins with Other *Fusarium* Toxins on Weaned Piglets: Membrane Lipids and Clinical Chemistry Approach. GINOP Conference 2021, Kaposvár, Hungary, 15 December, 2021.

7.5.1.3. **Ali O,** Mézes M, Balogh K, Kovács M, Szabó A. Effects of Fumonisins with Other *Fusarium* Toxins on Weaned Piglets: Membrane Lipids and Clinical Chemistry Approach. GINOP Conference 2021, Kaposvár, Hungary, 15 December, 2021.

7.5.1.4. Szabó A, Nagy S, **Ali O**, Gerencsér Z, Mézes M, Balogh KM, Bartók T, Horváth L; Mouhanna A, Kovács M. Effects of Fumonisin B Series on the Male Rabbit Reproductive

System: Testicular and Spermatological Investigations. 29th Animal Science Day International Symposium, Gödöllő, Hungary, 13-17 September, 2021.

7.5.1.5. Ali O. Subchronic exposure to fumonisin exerts negligible effects on the reproductive system of adult male buck. Elektronikus PhD Hallgatói és Oktatói Workshop az állattenyésztési kutatások területén, Kaposvár, Hungary, 4 May, 2021.

7.5.1.6. Ali O, Szabó A, Kovács M. The effects of oral fumonisin B1 exposure on the renal and hepatic lipid metabolism. 17th Global Toxicology and Risk Assessment Conference, Budapest, Hungary; 22-24 October, 2018.

7.5.2. Posters

7.5.2.1. Ali O, Mézes M, Balogh KM, Kovács M, Szabó A. Fumonisin B Series' Effects on the Lung Membrane Lipids of Piglets. TOX'2022 Tudományos Konferencia, Zalakaros, Hungary, 12-14 October, 2022.

7.5.2.2. Szabó A, **Ali O,** Lóki K, Balogh K, Mézes M, Bartók T, Horváth L, Kovács M. Sensitivity of the porcine hepatic cell membrane to fumonisin B1 during short exposure period. MycoKey-MycoTWIN Conference 2021, Bari, Italy, 9-12 November, 2021.